Available online at www.sciencedirect.com
SCIENCE DIRECT®
Journal of Chromatography A, 1052 (2004) 103–110
JOURNAL OF CHROMATOGRAPHY A
www.elsevier.com/locate/chroma

Chromatographic behavior of pyrithiones

Caren Anja Doose[a,*], Maciej Szaleniec[b], Peter Behrend[a], Anja Müller[a], Bernd Jastorff[a]

[a] *Center for Environmental Research and Environmental Technology, Department for Bioorganic Chemistry, University of Bremen, P.O. Box 330440, D-28334 Bremen, Germany*
[b] *Institute of Catalysis and Surface Chemistry, Polish Academy of Sciences, Krakow, Poland*

Received 24 May 2004; received in revised form 10 August 2004; accepted 10 August 2004

Abstract

Pyrithione biocides are currently viewed as a major prospect for the replacement of tributyltin antifoulants in ship paints. The chromatographic behavior of 1-hydroxy-2-pyridinethione (pyrithione, PT), bis(2-pyridinyl)disulfide 1,1′-dioxide (PT_2), and the metal complexes zinc [$Zn(PT)_2$], iron [$Fe(PT)_3$] and copper [$Cu(PT)_2$] pyrithione, were investigated by means of UV–vis spectroscopy, ESI-MS^n, HPLC-DAD and HPLC-ESI-MS^nD. This revealed transformations of the analytes, which affect the development of adequate methods for species or environmental analysis of pyrithiones. PT transforms into copper- or iron- containing complexes and/or the oxidation product PT_2, depending on the type of the stationary phase used in chromatographic analysis. Speciation complicates direct chromatography of [$Zn(PT)_2$] and [$Fe(PT)_3$].
© 2004 Elsevier B.V. All rights reserved.

Keywords: Pyrithione; Omadine; Zinc pyrithione; Antifouling biocides; Speciation

1. Introduction

1-Hydroxy-2-pyridinethione **1**, known as pyrithione (PT) or Omadine® (Table 1), has been noted for its highly bacteriocidal and fungicidal action for more than 50 years [1–3]. PT is a bidentate ligand that forms stable complexes with most transition metals [4–6]. Metallization of PT often results in highly augmented biocidal action as in the case of zinc pyrithione **2** [$Zn(PT)_2$] [1], which is the most commonly produced PT derivate and a well-known industrial chemical. [$Zn(PT)_2$] is used as a preservative in a broad spectrum of commercial products, from rubbers and industrial fluids to cosmetics. It is also an effective antidandruff agent, and has been employed in several hair care products for the last 30 years (e.g., Head & Shoulders®, Dove®). Moreover, pyrithione possesses a broad action against marine organisms, and it therefore also finds application as a booster biocide in anti-fouling paints [7–9].

Due to the ban on organotin antifoulants in ship paints established by the International Maritime Organization (IMO), the use of substitute biocides is of increasing importance. For example, Arch Chemicals, producers of [$Zn(PT)_2$] announced substantial production growth for 2002 and expected to become leaders in the antifouling biocide market by 2003 or 2004 [10].

This increases the necessity of risk assessment of a large-scale release of pyrithione biocides into the natural environment. Risk assessment calls not only for environmental fate studies of [$Zn(PT)_2$], it also requires the knowledge and understanding of the biological action of pyrithione biocides since they have been shown to affect non-target organisms at very low concentrations.[1] Therefore, methods for pyrithione analysis are needed. They are indispensable,

* Corresponding author. Present address: Department of Chemistry, School of Engineering and Science, IUB – International University Bremen, Campus Ring 8, D-28759 Bremen, Germany.
E-mail address: c.doose@iu-bremen.de (C.A. Doose).

[1] Early life stage tests exhibited significant teratogenic effects (morphologically visible wavy structures of the vertebral column) at very low concentrations of [$Zn(PT)_2$] in larvae of zebra fish and Japanese Medaka [11].

0021-9673/$ – see front matter © 2004 Elsevier B.V. All rights reserved.
doi:10.1016/j.chroma.2004.08.028

Table 1
Pyrithiones

Molecular structure	Chemical name	Abbreviation	No.
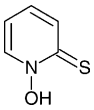	Pyrithione	PT	**1**
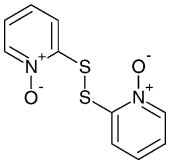	Bis(2-pyridinyl)disulfide 1,1′-dioxide	PT_2	**3**
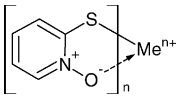	Zinc(II)-	$[Zn(PT)_2]$	**2**
	Copper(II)-	$[Cu(PT)_2]$	**4**
	Iron(III)-	$[Fe(PT)_3]$	**5**
Me = Zn^{2+}, Cu^{2+}, Fe^{3+}	Pyrithione		

on the one hand, for monitoring the occurrence of $[Zn(PT)_2]$ and its transformation products in natural environments, and, on the other hand, for species analysis of pyrithiones in physiological media, in order to elucidate the molecular mechanisms that determine the biological action of pyrithiones.

Several publications have already been dedicated to the chromatographic analysis of pyrithiones in commercial products or in biological media [13–23]. It is well known that reactions of the analytes with parts of the analytic device – these reactions have not been further specified – complicate the chromatography of pyrithiones [18–22]. The analysis of environmental samples is thus of limited reliability. Online trans-metallization of $[Zn(PT)_2]$ with copper(II) and subsequent measurement of generated $[Cu(PT)_2]$, which is a more stable complex than $[Zn(PT)_2]$ [21–23], suffers from low recovery rates and reproducibility [24]. To date, the American Society for Testing and Materials (ASTM) has not approved any analytical method for pyrithiones, although engaged in testing such methods for some time. This and the difficulties encountered in previous studies might be due to the delicate chromatographic behavior of pyrithiones illustrated herein.

In order to develop the methods for environmental or species analysis for delicate analytes such as pyrithiones it is crucial to understand the molecular mechanisms causing the analytical difficulties. The aim of the present study is to illustrate the complexity of pyrithione analysis and to elucidate its chromatographic behavior in order to guide the development of a reliable pyrithione analysis into the right direction. Additionally, the chromatographic behavior provides valuable information on chemical properties of pyrithiones that might also determine their behavior, e.g., in environmental or physiological media.

We investigated the chromatographic behavior of PT, $[Zn(PT)_2]$ and structural analogues, namely bis(2-pyridinyl)disulfide 1,1′-dioxide **3** (pyrithione disulfide, PT_2), copper **4** $[Cu(PT)_2]$ and iron **5** $[Fe(PT)_3]$ pyrithione (Table 1). These compounds are potential transformation products of PT and $[Zn(PT)_2]$ as will be discussed later. The chromatographic behavior of pyrithiones was investigated by means of HPLC-DAD, HPLC-ESI-MS^nD as well as offline UV–vis and ESI-MS^n.

2. Experimental

2.1. Chemicals

1-Hydroxy-2-pyridinethione **1** (pyrithione, PT) 99% was purchased from Aldrich (Germany). Purity of the standard was verified by ^1H and ^{13}C NMR. In order to prevent oxidation freshly obtained PT was handled under carbon dioxide atmosphere. *Zinc pyrithione* **2** $[Zn(PT)_2]$ 95% was purchased from Sigma (Germany). *Bis(2-pyridinyl)disulfide 1,1′-dioxide* **3** (PT_2) 99% was synthesized as described in [25] and characterized by UV and ESI-MS. *Copper* and *iron pyrithione* **4** $[Cu(PT)_2]$ and **5** $[Fe(PT)_3]$ were obtained as described in [26] and characterized by ESI-MS, UV–vis. In the case of $[Fe(PT)_3]$ X-ray diffraction measurements were performed in addition. For calculations of capacity factors K', the hold-up time (t_0) was determined with *uracil* 99+% (Acros, Germany). *UV–vis and*

$[Zn(PT)_2]$ exhibited EC_{50} values of 9 μg/L (28 nM) in zebra fish and 5 μg/L (16 nM) in Japanese Medaka. Kobayashi and Okamura [12] comparatively assessed the effects of tributyltin oxide and seven organotin antifoulant substitutes on sea urchin eggs and embryos. With no observed effect concentrations (NOEC) of 0.03 attoM $[Zn(PT)_2]$ was the most toxic antifoulant tested. $[Cu(PT)_2]$ exhibited a NOEC value of 3 femtoM.

HPLC solvents: gradient-grade methanol was obtained from Riedel (Germany), deionized water was further purified with a Milli-Q® Water Purification System (Germany), and formic acid puriss. p.a. grade was purchased from Fluka (Germany).

2.2. Apparatus

Offline UV-spectra: all samples were dissolved in mobile phase (for composition of the mobile phase please refer to the section on chromatographic conditions). The spectra were recorded against a mobile phase background with a Beckman DU® 640 spectrometer (Germany). (A solvent cut-off due to formic acid was observed for wavelengths lower than λ = 225 nm.) *Offline ESI-MS^n spectra*: the samples were prepared in mobile phase and analyzed by syringe pump injection with the same detector that was used for HPLC-ESI-MS^{n}D. *HPLC-DAD and HPLC-ESI-MS^{n}D*: the chromatographic analyses were performed on two HP 1100 Series® HPLC Systems (Germany) with binary pump and auto sampler, one incorporating a ColComp diode array detector, another an Agilent 1100 Series® VWD coupled with an Esquire-LC® ESI-ion trap detector (positive polarity). The results were analyzed with HP LC/MSD ChemStation. The HPLC columns used in this study were: LiChrosorb® RP-18 (Merck KGaA, Germany), 10 μm, 250 mm × 4.6 mm packed in-house, Chromolith Performance® RP-18e (Merck KGaA, Germany), 100 mm × 4.6 mm, Chromolith SpeedROD® RP-18e (Merck KGaA, Germany), 50 mm × 4.6 mm, Nucleosil® 100-5 C18 HD (Agilent Technologies, Germany), 125 mm × 2 mm prepacked, EcoCART LiChrospher® RP-select B (Merck KGaA, Germany), 5 μm, 125 mm × 3 mm prepacked, Polyspher® RP-18 (Merck KGaA, Germany), 150 mm × 4.6 mm prepacked, Purospher STAR® RP-18e (Merck KGaA, Germany), 5 μm, 250 mm × 2 mm prepacked, Kromasil® RP-18 (EKA Chemicals, Germany), 10 μm, spheric, 250 mm × 4.6 mm packed inhouse, and MetaSil Basic® RP-8 (Varian, Germany), 5 μM, 250 mm × 4.6 mm prepacked.

2.3. Chromatographic conditions

If not described otherwise the analyses were performed using an isocratic 30% methanol/70% water mobile phase containing 0.175% formic acid in the aqueous portion at room temperature and a flow rate of 1.0 mL/min (injection volumes and concentrations as noted). Duplicates were performed for each injection.

2.4. Isotope patterns calculation

For identification of MS signals isotope patterns were calculated with the Sheffield ChemPuter isotope patterns calculator [27].

3. Results

In order to identify the eluating solutes, UV–vis spectra were taken offline from each analyte in advance of chromatography. In the case of PT care had to be taken that spectra were obtained from fresh material which was handled under carbon dioxide atmosphere. Unprotected solid PT or aqueous solutions of PT were found to partially oxidize yielding the corresponding disulfide PT_2 (Fig. 8). The UV spectra of PT, PT_2, $[Zn(PT)_2]$, $[Cu(PT)_2]$ and $[Fe(PT)_3]$ are shown in Fig. 1. Additionally, offline ESI-MS spectra were taken from the individual compounds in order to identify the eluating solutes (only key data are included in this article).

3.1. Pyrithione

Chromatography of freshly prepared PT on LiChrosorb® RP-18 gave the chromatogram shown in Fig. 2(a). The recorded DAD plot of this run exhibited no fraction with the typical PT absorbance (Fig. 2(b)). Instead, the first signal at 3.22 min exhibited the spectrum of PT_2. A second signal came after 7.17 min exhibiting the spectrum of $[Cu(PT)_2]$ (Fig. 2(b) and (c)).

In order to test whether the reactions took place on stainless steel parts of the HPLC device (e.g., the injection valve or capillaries) or in the chromatographic column, the same sample was injected after removing the column from the device. This produced the original PT absorption pattern and thus ensured that the reactions happened in the column. Re-

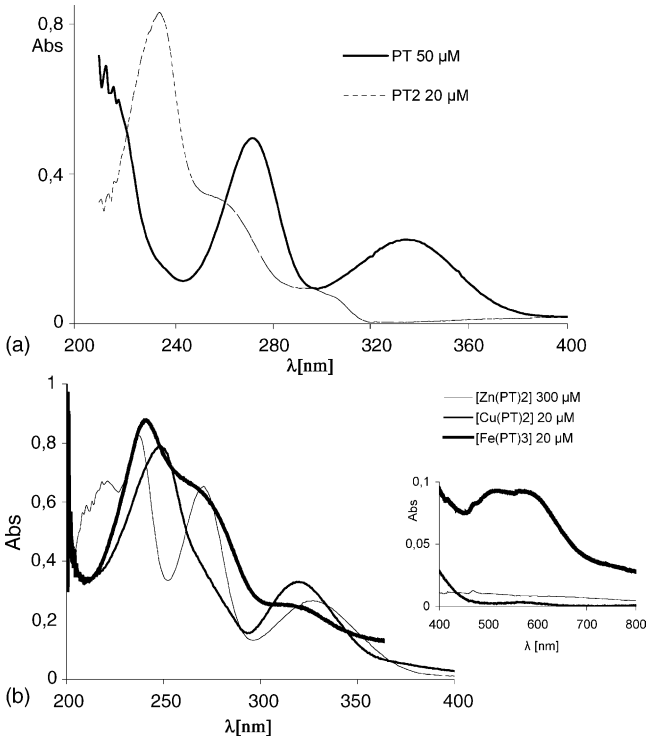

Fig. 1. UV spectra of (a) PT and PT_2, and (b) $[Zn(PT)_2]$, $[Cu(PT)_2]$, and $[Fe(PT)_3]$.

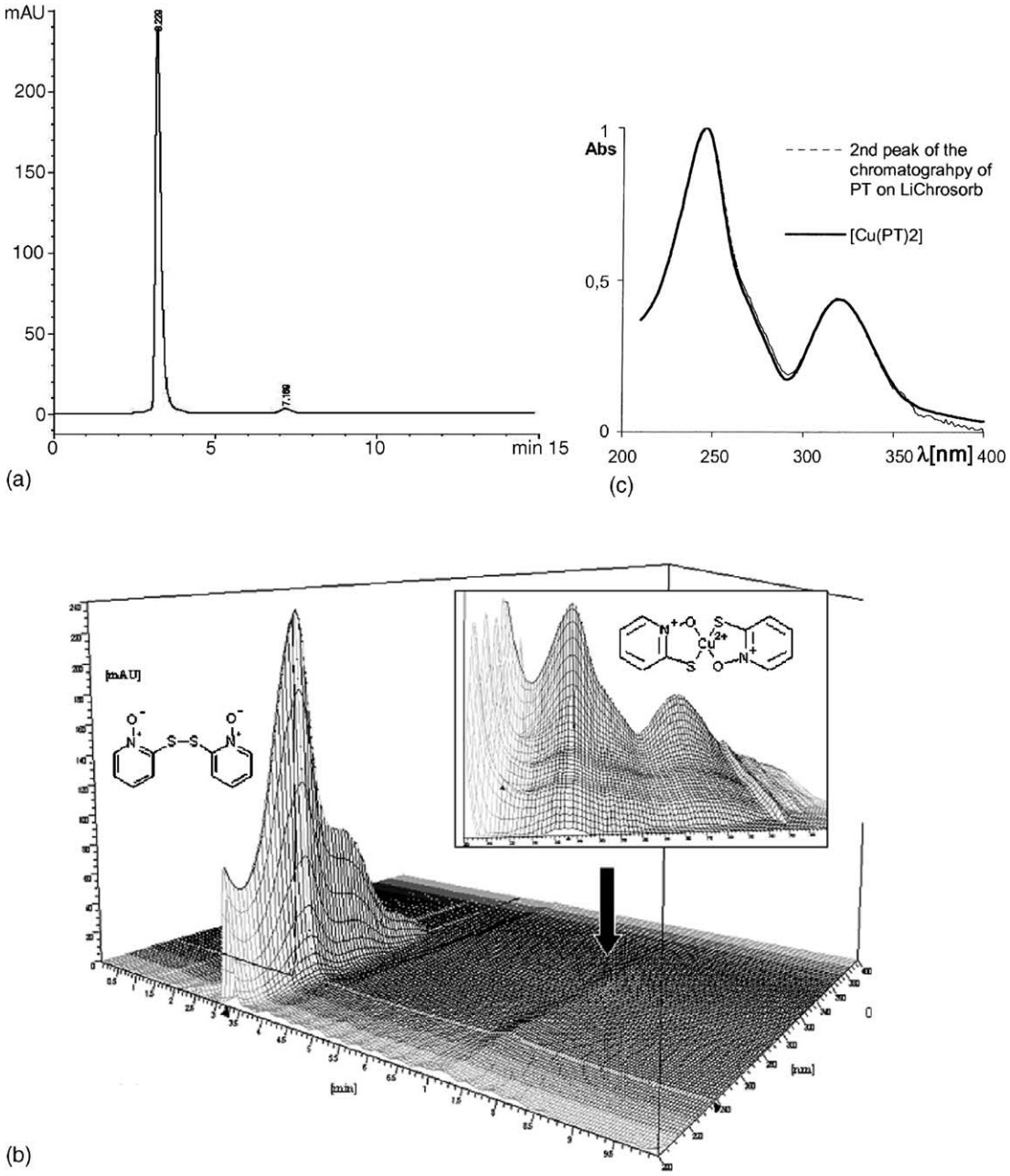

Fig. 2. Pyrithione on LiChrosorb® RP18 (2,5 μL, 2.5 mM): (a) single wavelength plot, (b) 3D plot, and (c) UV spectrum of the second signal of the chromatography of PT on LiChrosorb® in comparison to the UV spectrum of $[Cu(PT)_2]$ (both normalized to one).

placement of both stainless steel frits of the column by small disks of glass wool then proved that the reactions took place in the stationary phase since this had no influence on the transformation of PT.

Chromatography of PT on Polyspher®, EcoCART®, Purospher®, Purospher STAR®, LiChrosorb®, Metasil® and Nucleosil® lead to similar results (Table 2). When columns declared as metal free were employed only the disulfide was detected. From other columns either metal complex and disulfide or only metal complex eluated. Chromolith Performance®, Chromolith SpeedROD® and Kromasil RP-18® (Fig. 3) emerged as the only columns in this study that

Table 2
Observed transformations after injection of PT

Column	Transformations
Chromolith Performance® RP-18e	No transformation observed
Chromolith SpeedROD® RP-18e	No transformation observed
EcoCART LiChrospher® RP-select B	Metallization
Kromasil® RP-18	Partial metallization
LiChrosorb® RP-18	Oxidation and metallization
MetaSil Basic® RP-8	Oxidation
Nucleosil® 100-5 C18 HD	Metallization
Polyspher® RP-18	Oxidation and metallization
Purospher STAR® RP-18e	Oxidation

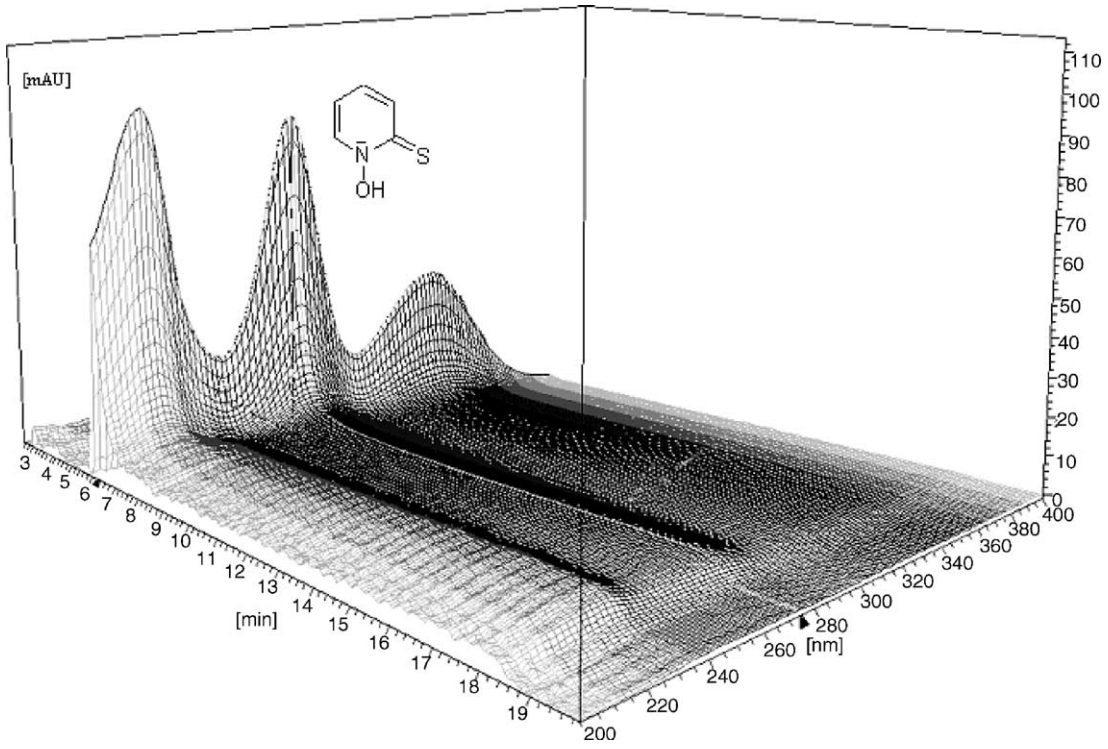

Fig. 3. Pyrithione on Kromasil® (10 μL, 1 mM), 3D plot.

do not completely interfere with PT so that the typical absorptions of PT could be observed in the eluate. Experiments exhibited that these three columns showed no differences in peak intensity, peak shape and retention time after 10 consecutive injections. Chromolith® columns exhibited peaks for PT of high symmetry, but the retention times for PT were very low even at a methanol concentration of 5% (K' = 3.1). These columns would therefore not allow for separation from more polar compounds. Kromasil® RP 18, which exhibited higher retention times (e.g., K' = 1.5 for 30% methanol in the mobile

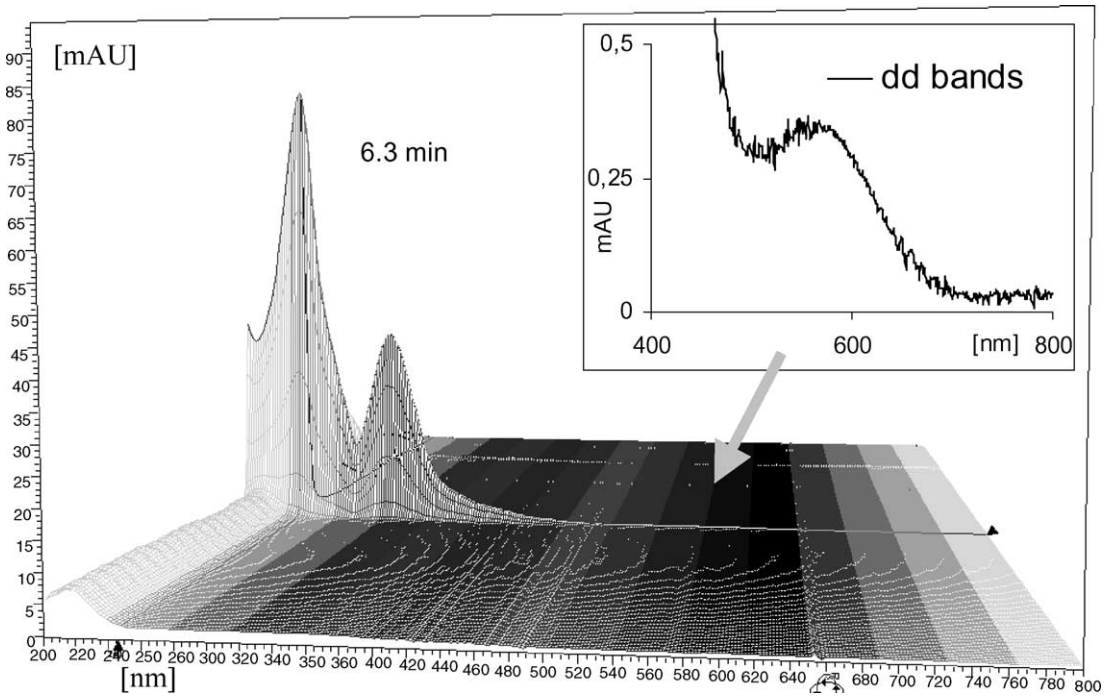

Fig. 4. [Cu(PT)$_2$] on Kromasil (30 μL, 0.29 mM; 60% methanol/40% water, formic acid (0.175%)).

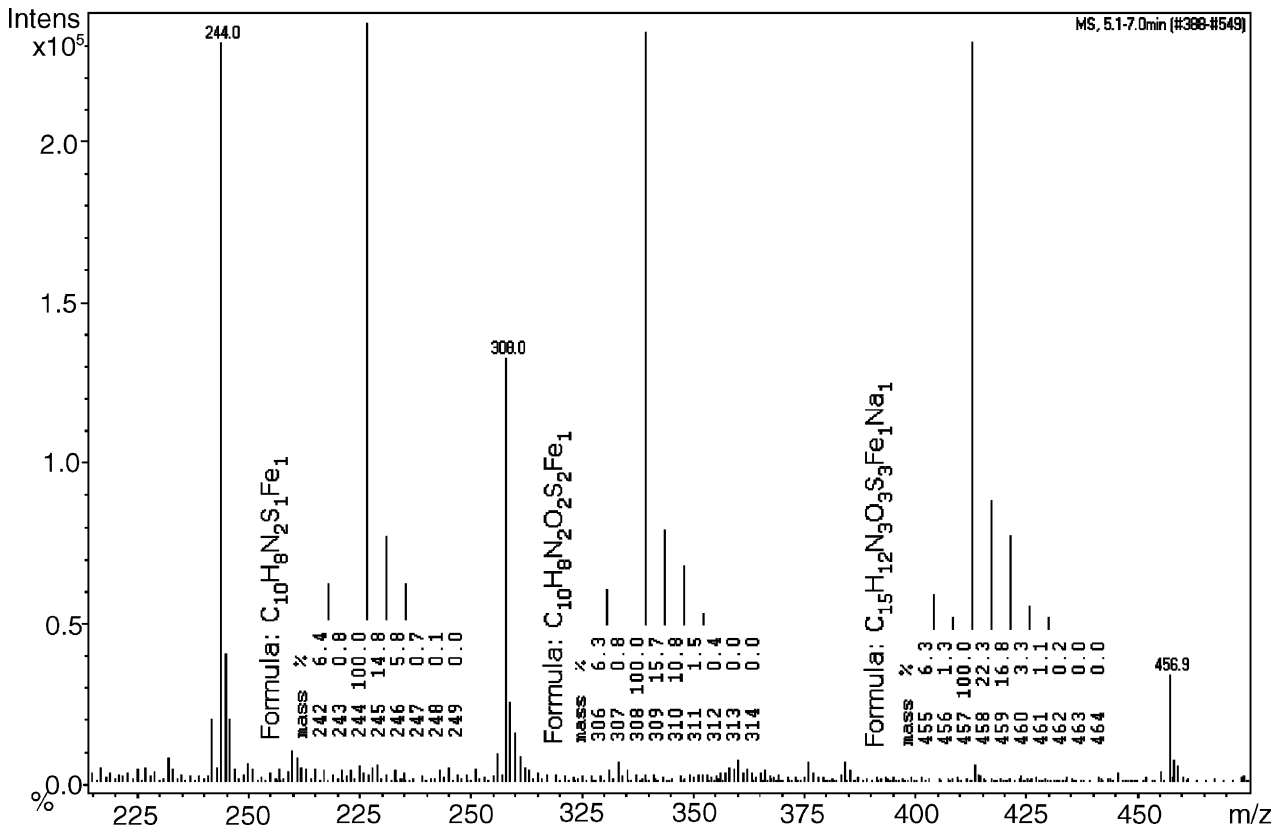

Fig. 5. Summarized MS signals (5.1–7.0 min fraction) of the chromatography of [Fe(PT)$_3$] in comparison with the results of the isotope patterns calculation.

phase), was chosen for further investigations, although tailing of the PT signal was observed on this material. It nevertheless allowed for qualitative PT identification. The tailing exhibited ESI-MS signals and UV–vis absorbances, which were identified as iron-containing compounds. The same signals have been found in the chromatography of [Fe(PT)$_3$] (Fig. 5).

3.2. [Cu(PT)$_2$]

Due to its late eluation a higher methanol concentration was used in the mobile phase for the chromatography of [Cu(PT)$_2$]. The 3D plot of [Cu(PT)$_2$] is shown in Fig. 4. [Cu(PT)$_2$] dd-transitions of the complex are present at 570 nm.

3.3. [Fe(PT)$_3$]

The HPLC analysis of the iron(III) complex of PT turned out to be difficult. The low solubility of [Fe(PT)$_3$] in water results in very low peak intensities. At 50% and higher methanol portions in the mobile phase peak intensities were sufficient but the [Fe(PT)$_3$] fractions eluated too fast and separation could not take place. The eluating fractions were very broad and exhibited UV–vis spectra different from the original sample while the CT bands characteristic for the complex could be observed in most all fractions. The HPLC-ESI-MS^{n}D of the eluate showed three characteristic signals (Fig. 5). The comparison with calculated isotope patterns confirms the identification of [Fe(III)(PT)$_2$-SO$_2$]$^+$ for *m/z* = 244, [Fe(III)(PT)$_2$]$^+$ for *m/z* = 308, and [Fe(III)(PT)$_3$+Na]$^+$ for *m/z* = 457.

3.4. [Zn(PT)$_2$]

An injection of [Zn(PT)$_2$] via syringe pump directly into the detector resulted in signals with isotope patterns in accordance with those calculated (Fig. 6). However, no zinc was found in the whole eluate of the HPLC-MS of [Zn(PT)$_2$] whereas pyridine-2-thione, PT$_2$ and iron complex species were observed.

[Zn(PT)$_2$] and [Fe(PT)$_3$] were also tested on some of the other columns, but the results were similar to those presented here, whereas [Cu(PT)$_2$] exhibited adequate signals on most of the columns tested.

4. Discussion

The present study revealed the complexity of the chromatographic behavior of pyrithiones. PT proved to oxidize on the stationary phases of many chromatographic columns yielding PT$_2$. The resulting disulfide signal does not show large broadening, and this suggests that the online generation of disulfide occurs quickly. Pyrithiones were also subject to (trans-) metallization reactions affording copper or iron-

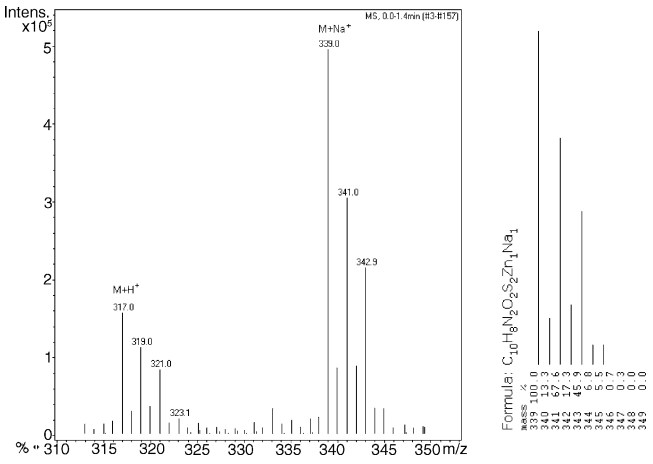

Fig. 6. Isotope patterns of $[Zn(PT)_2]$ received after injection via syringe pump in comparison with the result of isotope pattern calculation for the sodium adduct of $[Zn(PT)_2]$.

containing compounds. The transformations were found not to happen on metal parts of the chromatographic device such as capillaries and injection valve but on the stationary phase. According to the results presented here, oxidation and (trans-) metallization might be the mechanisms that currently complicate chromatographic analysis of pyrithiones also in other studies.

Six of nine columns completely transformed PT. No PT was found in the eluate of these columns. Only eluates from Chromolith Performance® and Chromolith SpeedROD® exhibited the UV–vis absorbance of this compound. These metal-free columns showed that it is principally possible to develop stationary phases that do not interfere with PT. The use of Chromolith® columns for PT analysis however is inadequate due to short retention times of PT. Kromasil® exhibited tailing of the PT signal, which was due to transformation yielding iron-containing species. Nevertheless, qualitative identification of PT and separation from PT_2 and other impurities was possible with this column. PT_2 and $[Cu(PT)_2]$ showed no transformation during chromatography on Kromasil®.

$[Zn(PT)_2]$ and $[Fe(PT)_3]$ could not be identified by means of HPLC-DAD and HPLC-ESI-MS^nD with any column employed. $[Zn(PT)_2]$ completely transformed during chromatography resulting in iron-containing species and PT_2. $[Fe(PT)_3]$ gave broad, not separated signals of iron- containing pyrithione species different from the original compound. The chromatographic behavior of both $[Zn(PT)_2]$ and $[Fe(PT)_3]$ can be explained with complex speciation (Figs. 7 and 8). This speciation was postulated and calculated in [28] (see also [26]) for $[Zn(PT)_2]$ by means of the Mass Law and the Henderson–Hasselbalch equation. According to this calculation, $[Zn(PT)_2]$ forms different portions of pyrithione species and free zinc(II) at micromolar concentrations, the pyrithionate **1a** exhibiting the largest portion. In the mobile phase the sample is being permanently diluted, causing further speciation, and each species possesses different retention times in the stationary phase. This results in peak broadening and loss of the zinc(II) moiety. $[Fe(PT)_3]$ might be subject to a similar speciation.

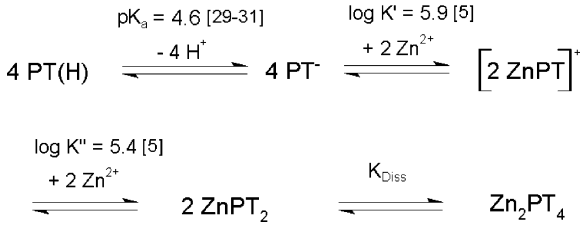

Fig. 7. Equilibria of $[Zn(PT)_2]$ [28–31].

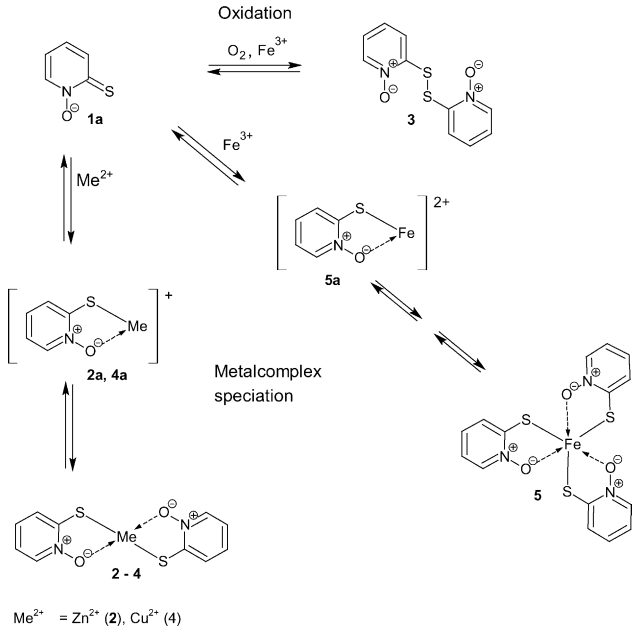

Fig. 8. Observed transformations of pyrithiones on stationary phases in HPLC.

The transformations of pyrithiones identified on stationary HPLC phases are summarized in Fig. 8.

5. Conclusion

The combined use of HPLC-DAD, HPLC-ESI-MS^nD and offline detection of UV–vis spectra has proven to be an adequate approach for the elucidation of the reactions of pyrithiones in the chromatographic system. This study clearly demonstrated that the sole use of fixed or variable wavelength detectors or mass detectors is not sufficient for the method development for the analysis of labile compounds. Transformation is not always seen as a broad signal, fronting or tailing, and the detection of only one wavelength does not provide univocal information on the analyte. Fragmentation and/or redox reactions of the analyte in the mass detector may obscure the identity of the solute as it leaves the column. Without DAD possible transformations of analytes according to those

described herein can be easily overlooked. This may have happened in previous studies.

Principally, analysis of pyrithione via HPLC might be possible. However, the stationary phase not only must be metal-free; the proneness of pyrithione to oxidation requires that the redox potential of the sationary phase is lower than that of the analyte. The material used for Chromolith® columns appears appropriate to avoid both oxidation as well as trans-metallization. However, in order to obtain adequate retention times the column should be more polar/less hydrophobic. Phenyl derivatized stationary phases could also constitute appropriate tools for the analysis of pyrithiones as long as the other conditions mentioned herein are met. The approach of trans-metallization of $[Zn(PT)_2]$ to $[Cu(PT)_2]$ as described in [22] appears reasonable; the reasons for the difficulties encountered for this method noted in [24] remain obscure calling for further investigations.

It should be underlined that published methods for pyrithione analysis need to be revised in light of the present results. The same applies to environmental fate studies and risk assessments that rely on data obtained through these methods.

Since oxidants and metal cations like Cu(II) and Fe(III) are ubiquitous, the transformation products observed in the present study (PT_2, $[Fe(PT)_3]$ and $[Cu(PT)_2]$) are also potential environmental transformation products. Cupric and ferric ions are in particular present in high concentrations in shipping environments (shipping lanes, harbors). Cupric oxide is used as an additive in antifouling paints. As shown in [26], these compounds exhibit highly toxic potential. Their environmental occurrence and fate should therefore be investigated and monitored in order to validate sustainability of pyrithione antifoulants that has been recommended by manufacturers.

References

[1] J.G. Black, D. Howes, Clin. Toxicol. 13 (1) (1978) 1.
[2] W.T. Gibson, W.S. Hardy, M.H. Groom, Food Chem. Toxicol. 23 (1) (1985) 103.
[3] G.A. Hyde, J.D. Nelson Jr., Cosmetic Drug Preserv. (1984) 115.
[4] J. Sun, Q. Fernando, H. Freiser, Anal. Chem. 36 (13) (1964) 2485.
[5] A. Albert, C.W. Rees, A.J.H. Tomlinson, Br. J. Exp. Pathol. 37 (1956) 500.
[6] B.L. Song, Z.S. Lu, D.Z. Niu, Y. Cao, Chin. Chem. Lett. 1 (2) (1990) 117.
[7] Olin Corporation, Harmful effects of the use of anti-fouling paints for ships: environmental risk assessment of zinc pyrithione anti-fouling biocides, MEPC 42/5/10, International Maritime Organization, Marine Environment Protection Committee, 4 September 1998, http://www.imo.org/index.htm.
[8] N. Voulvoulis, M.D. Scrimshaw, J.N. Lester, App. Organomet. Chem. 13 (3) (1999) 135.
[9] D.E. Audette, R.J. Fenn, J.C. Ritter, G. Polson, P. A. Turley, The Euro-Mediterranean Centre on Insular Coastal Dynamics, Costs and Benefits, in: An International Conference on From Antidandruff to Antifoulant: A Non-Persistent Alternative to TBT and Alternative Antifoulants, Foundation for International Studies, Malta, 4–6 December 1995.
[10] R. Martin, PCI interview, Arch Chemicals, 20 September 2002, www.archbiocides.com/marine/news.asp.
[11] K. Goka, Environ. Res. 81 (1) (1999) 81.
[12] N. Kobayashi, H. Okamura, Mar. Pollut. Bull. 44 (2002) 748.
[13] H. Cheng, R. Gadde, J. Chromatogr. 291 (1984) 434.
[14] C. Mitoma, T. Steeger, J. Rogers, D. Thomas, J.H. Wedig, Fundam. Appl. Toxicol. 3 (4) (1983) 256.
[15] B. Steinbrech, K.H. Koenig, Z. Fresenius, Anal. Chem. 316 (7) (1983) 685.
[16] K.H. Koenig, G. Schneeweis, B. Steinbrech, Z. Fresenius, Anal. Chem. 316 (1) (1983) 13.
[17] A.R. Jeffcoat, W.B. Gibson, P.A. Rodriguez, T.S. Turan, P.F. Hughes, M.E. Twine, Toxicol. Appl. Pharmacol. 56 (1) (1980) 141.
[18] R.J. Fenn, M.T. Alexander, J. Liq. Chromatogr. 11 (16) (1988) 3403.
[19] V. Ferioli, C. Rustichelli, F. Vezzalini, G. Gamberini, Chromatographia 40 (11–12) (1995) 669.
[20] L. Gagliardi, G. Multari, G. Cavazzutti, D.D. Orsi, D. Tonelli, J. Liq. Chromatogr. Relat. Technol. 21 (15) (1998) 2365.
[21] K. Nakajima, M. Ohta, H. Yazaki, H. Nakazawa, J. Liq. Chromatogr. 16 (1993) 487.
[22] K.V. Thomas, J. Chromatogr. A 833 (1) (1999) 105.
[23] K. Nakajima, T. Yasuda, J. Chromatogr. 502 (1990) 379.
[24] Personal communication, 10 March 2004. In preparation for balloting, ASTM volunteers are currently editing analytical methods for the determination of leach rates of $[Zn(PT)_2]$ from antifouling coatings. The method described in [22] has been included in these studies. Results unpublished.
[25] D.H.R. Barton, C. Chen, G.M. Wall, Tetrahedron 47 (32) (1991) 6127.
[26] C. Doose, J. Ranke, F. Stock, U. Bottin-Weber, B. Jastorff, Green Chem. 6 (5) (2004) 259.
[27] http://www.shef.ac.uk/chemistry/chemputer/isotopes.html, 2004.
[28] C. Doose, Dr. rer. nat. Dissertation, Pyrithiones – from molecular structure to biological action – implementation of the T-SAR approach for the understanding of delicate analytes and versatile biocides, University Bremen, 2003.
[29] R.A. Jones, A.R. Katritzky, J. Chem. Soc. (1960) 2937.
[30] B. Lynch, M.R. Smyth, in: M.R. Smyth, J.G. Vos (Eds.), Voltammetric Determination of Some Heterocyclic Mercaptans, Elsevier Science, Amsterdam, 1986, p. 97.
[31] A.F. Krivis, E.S. Gazda, G.R. Supp, M.A. Robinson, Anal. Chem. 35 (8) (1963) 966.